

Infrared Spectroscopy of $\text{NaCl}(\text{CH}_3\text{OH})_n$ Complexes in Helium Nanodroplets

Ahmed M. Sadoon,^{†,‡} Gautam Sarma,[†] Ethan M. Cunningham,[†] Jon Tandy,[†]
Magnus W. D. Hanson-Heine,[§] Nicholas A. Besley,[§] Shengfu Yang,^{*,†} and Andrew M. Ellis^{*,†}

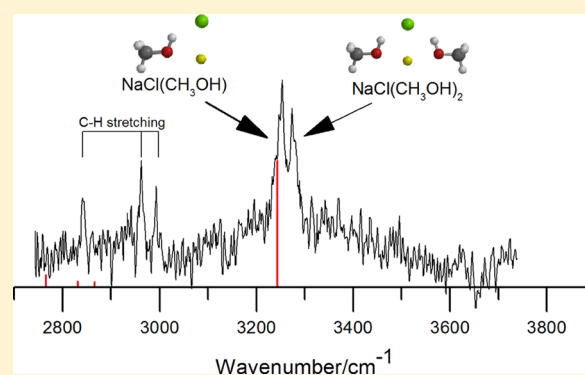
[†]Department of Chemistry, University of Leicester, University Road, Leicester LE1 7RH, United Kingdom

[‡]Department of Chemistry, College for Pure Sciences, University of Mosul, Mosul, Iraq

[§]School of Chemistry, University of Nottingham, University Park, Nottingham NG7 2RD, United Kingdom

S Supporting Information

ABSTRACT: Infrared (IR) spectra of complexes between NaCl and methanol have been recorded for the first time. These complexes were formed in liquid helium nanodroplets by consecutive pick-up of NaCl and CH_3OH molecules. For the smallest $\text{NaCl}(\text{CH}_3\text{OH})_n$ complexes where $n = 1-3$, the IR data suggest that the lowest-energy isomer is the primary product in each case. The predominant contribution to the binding comes from ionic hydrogen bonds between the OH in each methanol molecule and the chloride ion in the NaCl, as established by the large red shift of the OH stretching bands compared with the isolated CH_3OH molecule. For $n \geq 4$, there is a dramatic shift from discrete vibrational bands to very broad absorption envelopes, suggesting a profound change in the structural landscape and, in particular, access to multiple low-energy isomers.



INTRODUCTION

Alkali halides (MX) are archetypal univalent salts. The crystalline structure of the solid is disrupted by water, and these salts readily dissolve to form separated ions in dilute aqueous solutions. If the solid represents one extreme, then the counterpart is an isolated MX molecule. How might this smallest entity of salt, a single MX molecule, behave in the presence of a small water cluster, $(\text{H}_2\text{O})_n$? This problem can be addressed in experiments by forming isolated $\text{MX}(\text{H}_2\text{O})_n$ complexes and then using techniques, such as spectroscopy, to determine their properties. Such studies offer insight into the interaction between the constituent ionic particles and the solvent and can be reinforced through quantum chemical calculations. Understanding these interactions and the balance between them is critical in being able to carry out accurate simulations of bulk solutions.¹

An early infrared (IR) spectroscopic study of a $\text{NaCl}/\text{H}_2\text{O}$ mixture in an argon matrix provided a tentative assignment of vibrational bands of the $\text{NaCl}(\text{H}_2\text{O})$ complex.² The first detailed spectroscopic study of several different $\text{NaCl}(\text{H}_2\text{O})_n$ complexes ($n = 1-3$) was obtained by microwave spectroscopy, and this revealed important structural information.^{3,4} We have recently shown that complexes between NaCl and water molecules can be formed inside liquid helium nanodroplets, and this made it possible to record the first IR spectra of several small $\text{NaCl}(\text{H}_2\text{O})_n$ complexes.⁵ The spectra for $n = 1-3$ are consistent with structures in which an ionic hydrogen bond

(IHB) is formed between a single OH group in each water molecule and the Cl^- in the salt. Evidence for interwater hydrogen bonding only begins to appear for $n \geq 4$.

An alternative solvent to water is methanol. Most solid alkali halides will dissolve in methanol, but their solubility is far lower than that in water.^{6,7} The reduced solubility of salts in methanol when compared with that in water is a consequence of the hydrophobic (CH_3) group in the former. It would therefore be interesting to investigate how this amphiphilic character affects the interactions between a single salt molecule and one or more methanol molecules. It is well-known that addition of a salt to bulk water/alcohol mixtures causes a “salting-out” effect,⁸ in which the salt induces aggregation of the alcohol molecules and can bring about a phase separation into an aqueous salt phase and an alcohol/water phase. This phenomenon has some similarities to the salting-out effect associated with protein solubility in the Hofmeister series.⁹ There has been some controversy about how this phase separation happens. On the basis of neutron scattering measurements on NaCl in *t*-butanol, Bowron and Finney proposed that the salting-out effect is driven by a salt bridge consisting of a halide ion linking two alcohol molecules through two IHBs.¹⁰ However, Paschek et al. have rejected this suggestion and have instead presented both

Received: June 20, 2016

Revised: August 13, 2016

Published: September 29, 2016

experimental and theoretical evidence for an alternative mechanism in which a halide ion attaches to the methyl groups in *t*-butanol and thereby enhances the attractive interactions between the hydrophobic methyl groups in different *t*-butanol molecules.¹¹ These two explanations of the salting-out effect are clearly very different.

As a stepping stone to the study of the solvation of alkali halide molecules by more complex alcohols, as well as alcohol/water mixtures, we describe here the first IR spectroscopic study of NaCl(CH₃OH)_{*n*} complexes. The resulting data are consistent with the formation of contact ion-pair structures in which up to three methanol molecules can bind to an intact NaCl molecule, predominantly via IHBs between the OH groups and the chloride ion. These structures are analogous to the salt-bridge structures mentioned in the previous paragraph. For larger complexes, the narrow spectral bands are replaced with broad absorption features, which seem to arise from contributions from multiple low-energy conformers. In tandem with the experimental work, we employ quantum chemical calculations to explore the structural landscape of the complexes for $n \leq 4$.

■ EXPERIMENTAL SECTION

Full details of the apparatus and techniques employed here can be found in previous publications.^{5,12} In brief, helium nanodroplets with a mean size close to 5000 helium atoms were formed by expanding precooled gaseous helium into a vacuum through a 5 μm pinhole. The droplets then passed through two consecutive pick-up cells, the first containing NaCl vapor and the second methanol vapor. Gaseous NaCl was produced by resistively heating a pick-up cell containing solid sodium chloride. The temperature of this cell (445 °C) was chosen to ensure that most helium droplets contained no more than one NaCl molecule, as confirmed by recording mass spectra. Mass spectra of NaCl and its clusters in the gas phase have shown that the primary ion from NaCl is Na⁺, whereas that from the (NaCl)₂ dimer is Na₂Cl⁺.¹³ The NaCl vaporization conditions were therefore adjusted so that the Na₂Cl⁺ signal detected by electron ionization mass spectrometry was small relative to Na⁺ prior to addition of methanol in the second pick-up cell.

IR spectra were recorded via a depletion method that exploits the evaporative loss of helium atoms as the absorbed energy becomes dispersed into the droplet. This effect causes a decrease in the droplet size and therefore its geometric cross section, which can be registered by a drop in the signal identified via electron ionization mass spectrometry downstream of the IR excitation zone. In the current experiments, mass-selective ion detection has been used. This is important for two reasons: (1) by choosing appropriate ions, we can eliminate any contributions to the IR spectra from pure methanol and its clusters; (2) it provides a degree of size selectivity that aids spectral assignment, as detailed later. The line width of the optical parametric oscillator used to excite IR transitions is 4–5 cm⁻¹.

■ COMPUTATIONAL DETAILS

Calculations on NaCl(CH₃OH)_{*n*} for $n = 1–4$ were carried out using density functional theory (DFT) within the Q-Chem software package.¹⁴ Geometry searches, energy evaluations, and vibrational frequency calculations were performed using the M06 functional.¹⁵ In order to search through a wide range of

potential geometries, a total of 50 different initial configurations were generated by randomly rotating and translating each molecule within a 50 *a*₀³ box (*a*₀ = the atomic unit of length = 0.5292 Å), with the NaCl bond length fixed at 2.481 Å for $n = 1$, 2.607 Å for $n = 2$, 2.907 Å for $n = 3$, and 3.085 Å for $n = 4$, as the length of the NaCl bond is found to lengthen with the addition of extra methanol molecules. In order to avoid self-consistent field convergence problems, atoms in different molecules were prevented from becoming closer than 3 *a*₀ from each other. The initial configurations were then optimized without constraint (including variation of the Na–Cl distance) at the M06/6-31+G(d) level of theory with the default SG-1 integration grid. For the smaller $n = 1$ and 2 complexes, all structures were reoptimized at the M06/6-311++G(d,p) level with an EML-(150,770) integration grid. For the $n = 3$ and 4 complexes, only the structures within 50 kJ mol⁻¹ of the minimum-energy structure were reoptimized at the higher level of theory.

Harmonic vibrational frequencies were then calculated and scaled to account for anharmonicity. Scaling factors for harmonic frequency calculations are well-established, but these scaling factors represent an average over many different types of vibrational mode.¹⁶ In this work, we derive a system-specific scaling factor for the OH stretching modes of the NaCl(CH₃OH)_{*n*} complexes. This scaling factor is derived purely on the basis of reference to anharmonic vibrational frequency calculations, that is, there is no use of experimental data. The anharmonic frequency calculations were performed using second-order vibrational perturbation theory (VPT2), as well as the transition optimized shifted Hermite (TOSH) variation on VPT2¹⁷ for the lowest-energy NaCl(CH₃OH)_{*n*} ($n = 1$ and 2) complexes. Third- and fourth-order derivatives of the energy with respect to nuclear displacement were evaluated for up to two-mode couplings. The approach adopted used finite differences and employed analytical gradients produced from a step size of 0.5291 Å along each normal mode. Averaging over the three vibrational modes and two methods gives a scaling factor of 0.924 for NaCl(CH₃OH)_{*n*} complexes. This value is lower than standard values for the scaling factor,¹⁶ which suggests that the OH stretching mode in these complexes has a high degree of anharmonicity, which in turn may be a consequence of the ionic hydrogen bonding (see later). A similar analysis for a single methanol molecule gives a value of 0.948, which is closer to the standard values for scaling factors.

■ RESULTS AND DISCUSSION

1. Overview of the Experimental Results. Figure 1 shows an illustrative mass spectrum in which two series of peaks are highlighted, one assigned to (CH₃OH)_{*m*}H⁺ and the other to (CH₃OH)_{*m*}Na⁺. The (CH₃OH)_{*m*}H⁺ ions are derived from ionization of helium droplets containing only methanol clusters, while the (CH₃OH)_{*m*}Na⁺ ions are the products of ionization of helium droplets containing NaCl(CH₃OH)_{*n*} complexes, where $n \geq m$. We have previously seen loss of Cl atoms from ionization of NaCl(H₂O)_{*n*} complexes in helium droplets,⁵ and a parallel process must occur here for the ionization of NaCl(CH₃OH)_{*n*}. To record IR spectra, we monitored the IR-induced depletion of specific (CH₃OH)_{*m*}Na⁺ ions.

Figure 2 shows IR spectra recorded by monitoring the ion signals for $m = 1–4$. Bands with relatively narrow line widths are seen for $m = 1–3$ in both the OH stretching and CH

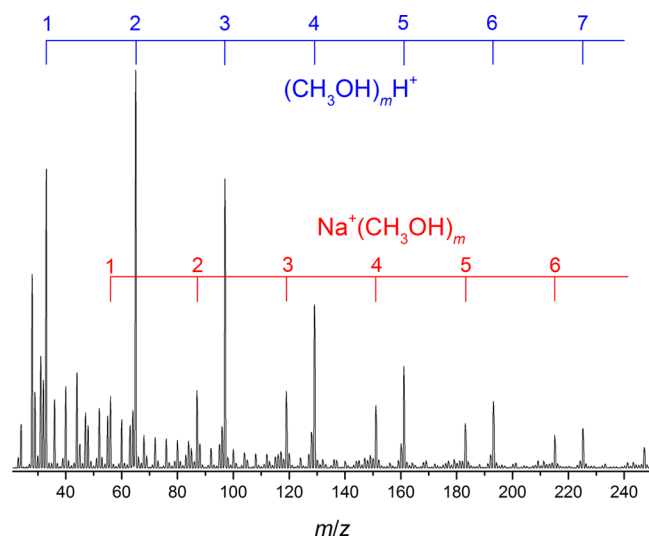


Figure 1. Mass spectrum from the NaCl/CH₃OH system obtained using an electron energy of 70 eV. Three series of ions are seen in this spectrum. Although not labeled in this figure, peaks from He_{*n*}⁺ cluster ions are particularly evident on the low mass side of the spectrum. The two labeled ion series correspond to (CH₃OH)_{*m*}H⁺ and (CH₃OH)_{*m*}Na⁺, where the former are derived from helium droplets containing only methanol molecules and the latter are derived from NaCl(CH₃OH)_{*n*} complexes.

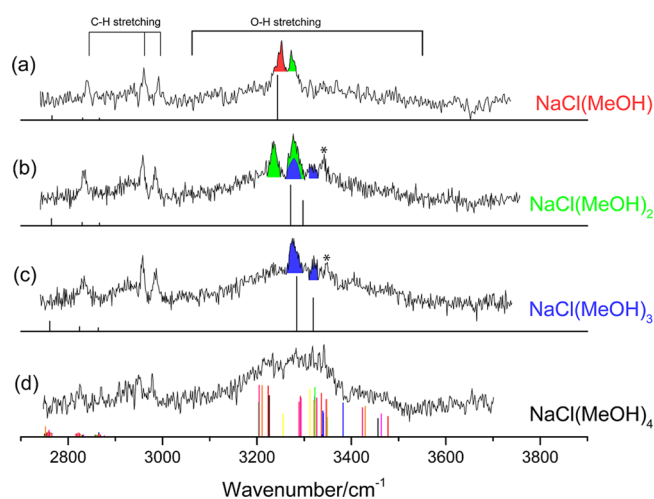


Figure 2. IR spectra of NaCl(CH₃OH)_{*n*} recorded by monitoring ion signals at (a) *m/z* 55 ((CH₃OH)Na⁺), (b) *m/z* 87 ((CH₃OH)₂Na⁺), (c) *m/z* 119 ((CH₃OH)₃Na⁺), and (d) *m/z* 151 ((CH₃OH)₄Na⁺). Also shown beneath the spectra in (a–c) are the predicted IR spectra for the global minimum-energy structures of *n* = 1–3, respectively, derived from DFT calculations. The asterisked peak in (b) and (c) is unassigned, as discussed in the main text. Beneath the spectrum in (d), we show the predicted IR bands for the *n* = 4 complex for the eight lowest energy structures, which all lie within 3 kJ mol^{−1} of the global minimum. The different colors represent different isomers, and their intensities have not been weighted by any assumed abundance distribution (see the main text for further details).

stretching regions. However, for *m* = 4, only a very broad OH stretching feature is seen, which reaches a maximum near 3300 cm^{−1}.

Before attempting to make specific IR band assignments, we first discuss the calculated structures for small NaCl(CH₃OH)_{*n*} complexes.

2. Predicted Structures. Four structures corresponding to distinct minima were found for the NaCl(CH₃OH) complex in the DFT calculations, all of which are shown in Figure 3. In the

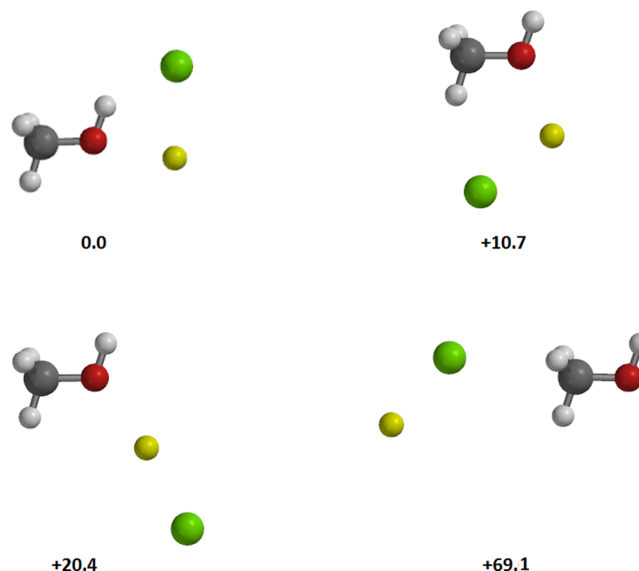


Figure 3. Calculated equilibrium structures for NaCl(CH₃OH) along with their energies (not corrected for zero-point energy) in kJ mol^{−1} relative to the global potential energy minimum.

global minimum, the NaCl ion pair is oriented so that the chloride ion (shown in green) can form an IHB with the OH, while additional stabilization is gained by the proximity of the Na⁺ ion (yellow) to the O atom (red). Similar behavior has been seen previously for NaCl(H₂O).^{4,5} In the next-lowest-energy minimum, which is 10.7 kJ mol^{−1} higher in energy than the global minimum, one of the C–H bonds points toward the chloride ion but in this case there is no IHB.

For NaCl(CH₃OH)₂, we have found five distinct minima (see Figure 4). The lowest-energy structure is analogous to the *n* = 1 complex but now has two IHBs linking the chloride ion and the OH groups. The next-lowest-energy minimum lies 2.9 kJ mol^{−1} above the global minimum and has two distinct bonding modes, one with methanol attached to the NaCl via an IHB. The other methanol molecule in this structure is oriented to allow partial interaction with both the OH group and one of the CH bonds from the methyl group.

For *n* = 3 and 4, the conformational landscapes are more complex. The global minimum for NaCl(CH₃OH)₃ is analogous to those found for NaCl(CH₃OH) and NaCl(CH₃OH)₂ but now with three equivalent IHBs (see Figure 5). However, other minima are more energetically accessible than those in the smaller complexes. In the lowest-energy structure for NaCl(CH₃OH)₄, one methanol molecule is no longer bound to NaCl via an IHB. Instead, this methanol is effectively in a second solvation shell and is hydrogen-bonded to one of the methanol molecules in the inner solvation shell (see Figure 6). However, there is a significant increase in the number of low-energy structures available for NaCl(CH₃OH)₄ when compared with NaCl(CH₃OH)₃.

3. Assignment of IR Spectra: OH Stretching. We start by considering bands in the OH stretching region. Here, there are several relatively narrow bands seen in Figure 2a–c obtained by detecting (CH₃OH)Na⁺, (CH₃OH)₂Na⁺, and (CH₃OH)₃Na⁺, respectively. Although we apply mass-selective

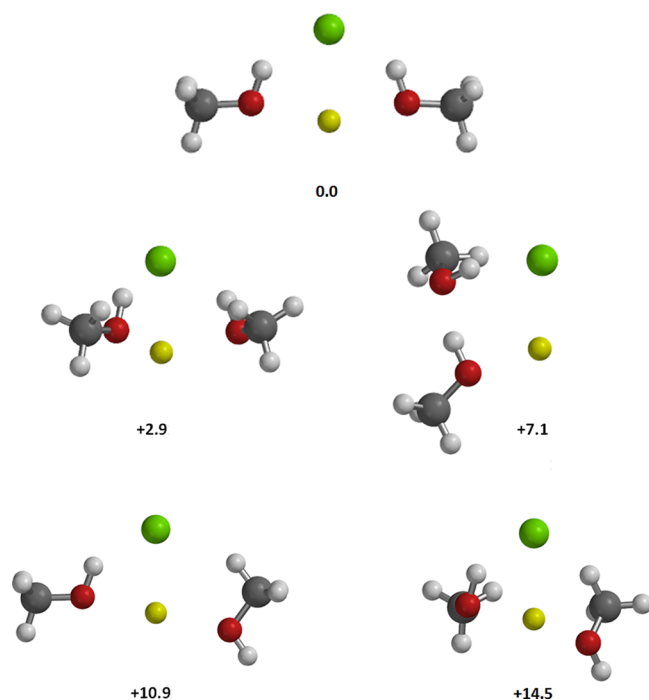


Figure 4. Calculated equilibrium structures for $\text{NaCl}(\text{CH}_3\text{OH})_2$ along with their energies (not corrected for zero-point energy) in kJ mol^{-1} relative to the global potential energy minimum.

detection of ions to record the IR depletion spectra, this does not guarantee spectral assignment of the neutral complex because ion fragmentation by loss of one or more methanol

molecules could lead to the same absorption band being seen in spectra from different mass channels. However, mass selectivity does make it possible to establish the *minimum* number of methanol molecules in the complex (or complexes) contributing to a particular IR spectrum.

We can also use the dependence of the IR signal on the methanol pick-up pressure to help establish n , and this was used previously to confirm the spectral assignments for $\text{NaCl}(\text{H}_2\text{O})_n$.⁵ Figure 7 shows pick-up pressure (PUCP) data for $\text{NaCl}(\text{CH}_3\text{OH})_n$. Also shown are Poisson curves for different values of n , which should describe the probability of picking up n dopant molecules in the limit of negligible droplet shrinkage after pick-up. Unfortunately, the PUCP measurements for $\text{NaCl}(\text{CH}_3\text{OH})_n$ are not as definitive as those for $\text{NaCl}(\text{H}_2\text{O})_n$, and there are two reasons for this. First, there are overlapping bands for different sized complexes, as will be evident by looking at Figure 2a–c, where peaks are seen at similar positions in different mass channels. Second, the relatively narrow OH stretching bands sit astride a broad underlying absorption feature, which we attribute to complexes with relatively large values of n (≥ 4). This quasi-continuous absorption is very obvious in the $(\text{CH}_3\text{OH})_2\text{Na}^+$ and $(\text{CH}_3\text{OH})_3\text{Na}^+$ mass channels in Figure 2, but there is even a contribution in the $(\text{CH}_3\text{OH})\text{Na}^+$ channel, and this grows as the partial pressure of methanol is increased. We can partially offset the effect of the broad absorption envelope by estimating and subtracting its contribution from the intensities of the narrower peaks as the methanol partial pressure is changed. However, the overlapping of the sharper bands restricts the information that can be extracted from PUCP data.

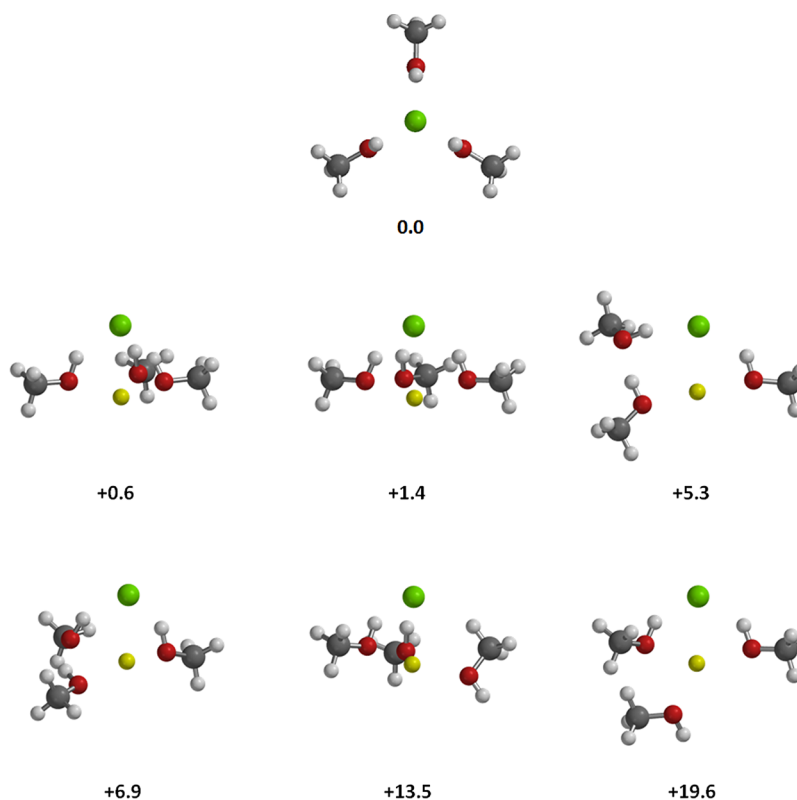


Figure 5. Calculated equilibrium structures for $\text{NaCl}(\text{CH}_3\text{OH})_3$ along with their energies (not corrected for zero-point energy) in kJ mol^{-1} relative to the global potential energy minimum. For the global minimum structure, the NaCl has been oriented with the Cl atom above the Na atom so as to show the trigonal (C_3 rotational) symmetry about the $\text{Na}-\text{Cl}$ bond axis.

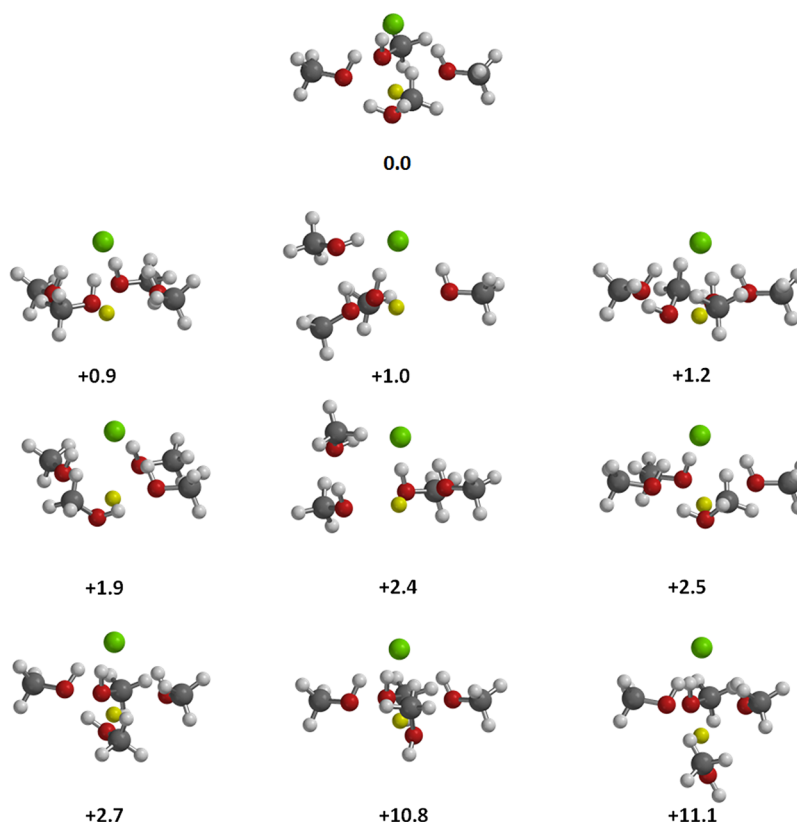


Figure 6. Calculated equilibrium structures for $\text{NaCl}(\text{CH}_3\text{OH})_4$ along with their energies (not corrected for zero-point energy) in kJ mol^{-1} relative to the global potential energy minimum.

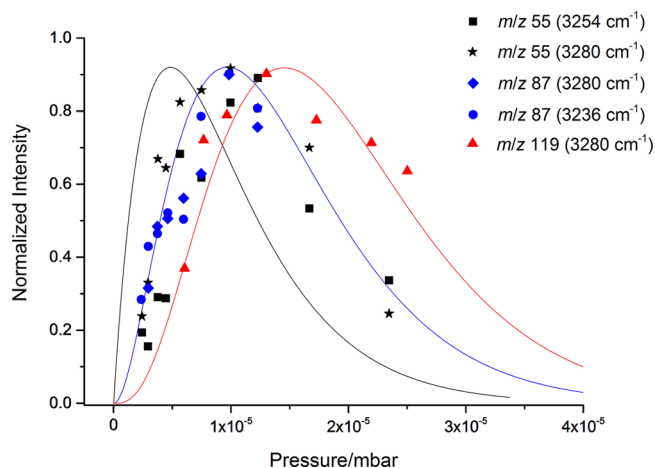


Figure 7. Dependence of the intensities of specific IR absorption bands, detected in the m/z 55 ($(\text{CH}_3\text{OH})\text{Na}^+$), m/z 87 ($(\text{CH}_3\text{OH})_2\text{Na}^+$), and m/z 119 ($(\text{CH}_3\text{OH})_3\text{Na}^+$) mass channels, on the partial pressure of methanol in the second pick-up cell. Also shown are the calculated Poisson curves for the pick-up of one (black), two (blue), and three (red) methanol molecules.

Before we attempt to make specific assignments, we note that the sharp bands in the OH stretching region, whose positions are summarized in Table 1, all lie between 3230 and 3360 cm^{-1} . This is a relatively narrow range, and the frequencies of these absorption bands are well to the red of the OH stretching band of the isolated methanol molecule.¹⁸ This red shift is characteristic of the formation of IHBs, which weaken the OH bonds and thereby lower the OH stretching frequencies. This effect has been seen previously in IR spectra of the anionic

Table 1. Positions and Assignments of OH Stretching Bands for $\text{NaCl}(\text{CH}_3\text{OH})_n$ for $n = 1-3$

band position	assigned carrier
3236	$\text{NaCl}(\text{CH}_3\text{OH})_2$
3254	$\text{NaCl}(\text{CH}_3\text{OH})$
3278	$\text{NaCl}(\text{CH}_3\text{OH})_2 + \text{NaCl}(\text{CH}_3\text{OH})_3$
3323	$\text{NaCl}(\text{CH}_3\text{OH})_3?$
3344	$\text{NaCl}(\text{CH}_3\text{OH})_3?$

$\text{Cl}^-(\text{CH}_3\text{OH})_n$ complexes, which have been studied in the gas phase by Lisy and co-workers.^{19,20} Clearly, there are some expected similarities between the interactions of methanol with Cl^- and NaCl given that the latter is a strongly ionic molecule, and therefore, we compare key features of their spectra here. For $\text{Cl}^-(\text{CH}_3\text{OH})_2$, two distinct structures were identified from the IR spectra: (1) one in which each methanol molecule is bound to Cl^- by an IHB and (2) a “two-shell” structure in which a methanol molecule binds to Cl^- by an IHB and then the second methanol molecule binds to the first by a normal hydrogen bond. The latter structure delivers a cooperatively enhanced IHB and results in an intense and hugely red-shifted band for this OH group, which appears at 2773 cm^{-1} .²⁰ We see no OH stretching bands with anything like such large red shifts and therefore conclude that in small $\text{NaCl}(\text{CH}_3\text{OH})_n$ clusters there is no hydrogen bonding between the methanol molecules. This distinction between $\text{Cl}^-(\text{CH}_3\text{OH})_n$ and $\text{NaCl}(\text{CH}_3\text{OH})_n$ most likely derives from the additional electrostatic stabilization provided by interaction between Na^+ and the O atom on methanol when an IHB forms with the chloride ion in NaCl (for example, see the global minimum-energy structure for $\text{NaCl}(\text{CH}_3\text{OH})$ in Figure 3). Structures with the maximum

number of IHBs will be energetically favored for small values of n .

We now attempt to make assignments for specific bands. We start by looking for the IR spectrum of the smallest complex, $\text{NaCl}(\text{CH}_3\text{OH})$. Taking into account possible ion fragmentation, the spectrum of this complex might be observable as signal depletion in the Na^+ or $(\text{CH}_3\text{OH})\text{Na}^+$ mass channels. Previously, we were able to record the IR spectrum of $\text{NaCl}(\text{H}_2\text{O})$ by detecting Na^+ .⁵ However, when H_2O is replaced by CH_3OH , there are no OH stretching features when detecting Na^+ (see the [Supporting Information](#)), and therefore, we conclude that ionization of $\text{NaCl}(\text{CH}_3\text{OH})$ in a helium droplet leads to ejection of Cl but is not accompanied by CH_3OH . Consequently, the IR spectrum of $\text{NaCl}(\text{CH}_3\text{OH})$ must lie within the scan recorded by detecting $(\text{CH}_3\text{OH})\text{Na}^+$, namely, [Figure 2a](#). This spectrum shows two partly overlapping bands, one peaking at 3254 cm^{-1} and the other at 3271 cm^{-1} , with the former being marginally stronger. Of these two bands, that at 3254 cm^{-1} has no exact counterpart in spectra from higher mass channels in [Figure 2](#), although it does partly overlap with a peak whose maximum is at 3236 cm^{-1} in the $(\text{CH}_3\text{OH})_2\text{Na}^+$ channel. Because the bands are relatively broad, with full widths at half-maximum $\geq 15\text{ cm}^{-1}$, an underlying contribution to the 3254 cm^{-1} band from a larger complex is inevitable. The PUCP curve for this band in [Figure 7](#) confirms this, showing a pressure dependence that is more in keeping with $n = 2$ than $n = 1$. Consequently, while we suspect that the peak at 3254 cm^{-1} has a contribution from IR absorption by $\text{NaCl}(\text{CH}_3\text{OH})$, this assignment must be seen as tentative. The other band seen in the $(\text{CH}_3\text{OH})\text{Na}^+$ mass channel, at 3271 cm^{-1} , is partly coincident with a band seen in both the $(\text{CH}_3\text{OH})_2\text{Na}^+$ and $(\text{CH}_3\text{OH})_3\text{Na}^+$ mass channels, which peaks at 3278 cm^{-1} . It is therefore possible that the 3271 cm^{-1} band in the $(\text{CH}_3\text{OH})\text{Na}^+$ channel is entirely an absorption band of $\text{NaCl}(\text{CH}_3\text{OH})_2$ and/or a larger complex, which fragments upon ionization.

Beneath the experimental spectrum in [Figure 2a](#) is a simulation of the IR spectrum derived from DFT calculations for the global minimum-energy isomer for $\text{NaCl}(\text{CH}_3\text{OH})$. If only this isomer is present in helium nanodroplets, then only a single OH stretching band is expected. The band assigned to $\text{NaCl}(\text{CH}_3\text{OH})$ in the IR spectrum is red-shifted by $\sim 430\text{ cm}^{-1}$ from the OH stretching band of the methanol monomer in superfluid helium,¹⁸ implying a very significant weakening of the O–H bond when methanol forms a complex with NaCl. This is consistent with the formation of an IHB between the OH and the chloride ion. The corresponding red shift for the anionic complex, $(\text{CH}_3\text{OH})\text{Cl}^-$, in the gas phase is 519 cm^{-1} .²⁰ The smaller red shift for $\text{NaCl}(\text{CH}_3\text{OH})$ when compared to the anion is reasonable for two reasons. First, the negative charge on the chloride ion in NaCl is expected to be smaller than that for bare Cl^- , making the IHB weaker. Second, electrostatic interactions between the Na and O atoms is also likely to modify the strength of the IHB. The experimental and DFT band positions in [Figure 2a](#) are in close agreement (the difference is 10 cm^{-1}), providing additional support for the assignment. Note that we can rule out contributions from other possible isomers shown in [Figure 3](#) because, in addition to being much higher in energy, they do not have IHBs and therefore will have OH stretching bands at much higher frequencies than those seen in [Figure 2](#) (see the [Supporting Information](#)).

The DFT calculations predict a global minimum-energy structure for $\text{NaCl}(\text{CH}_3\text{OH})_2$ in which each methanol molecule is independently bonded to the NaCl in a symmetrical configuration involving two IHBs. Consequently, symmetric and antisymmetric combinations of the two OH stretching vibrations will deliver two absorption bands. The sharing of Cl^- among two IHBs leads to a net weakening of each individual IHB when compared to $\text{NaCl}(\text{CH}_3\text{OH})$ because the negative charge is now shared between two IHBs. As a result, the O–H bonds strengthen and a smaller red shift for the OH stretches of $\text{NaCl}(\text{CH}_3\text{OH})_2$ versus $\text{NaCl}(\text{CH}_3\text{OH})$ is expected. The spectrum in [Figure 2b](#), recorded in the $(\text{CH}_3\text{OH})_2\text{Na}^+$ mass channel, shows two prominent bands of almost equal intensity, one centered at 3236 cm^{-1} and the other at 3278 cm^{-1} . The band at 3236 cm^{-1} has no counterpart in the spectrum recorded in the $(\text{CH}_3\text{OH})_3\text{Na}^+$ mass channel, and therefore, we assign it to $\text{NaCl}(\text{CH}_3\text{OH})_2$. This is supported by the corresponding PUCP curve in [Figure 7](#), which matches the Poisson curve for $n = 2$ quite closely. The DFT calculations predict a splitting of 26 cm^{-1} between the antisymmetric and symmetric OH stretches for the lowest-energy isomer of $\text{NaCl}(\text{CH}_3\text{OH})_2$. We therefore expect a second band at higher wavenumber, and it is likely that the band peaking at 3278 cm^{-1} has a contribution from $\text{NaCl}(\text{CH}_3\text{OH})_2$. However, a band is also seen at a similar position in the $(\text{CH}_3\text{OH})_3\text{Na}^+$ mass channel (see below), and therefore, the 3278 cm^{-1} band in [Figure 2b](#) probably has contributions from both $\text{NaCl}(\text{CH}_3\text{OH})_2$ and $\text{NaCl}(\text{CH}_3\text{OH})_3$. This seems to be supported by the PUCP data, which are somewhat scattered but fall between the Poisson curves for $n = 2$ and 3. Given this assignment, the splitting between the antisymmetric and symmetric OH stretching vibrations in $\text{NaCl}(\text{CH}_3\text{OH})_2$ is $\sim 42\text{ cm}^{-1}$, which is larger than the 26 cm^{-1} predicted from the DFT calculations. The central position between these two bands is shifted to the blue of the single OH stretching band of $\text{NaCl}(\text{CH}_3\text{OH})$, as expected, but the shift is only $+3\text{ cm}^{-1}$ whereas the DFT calculations predict a value of 41 cm^{-1} . Other isomers, such as the next-lowest-energy isomer at 2.9 kJ mol^{-1} above the global minimum, do not offer a better match with experiment (see the [Supporting Information](#)).

The strongest band in the $(\text{CH}_3\text{OH})_3\text{Na}^+$ mass channel peaks at 3278 cm^{-1} and was mentioned above because it overlaps with a band at a similar position in the $(\text{CH}_3\text{OH})_2\text{Na}^+$ mass channel. This band is assigned to $\text{NaCl}(\text{CH}_3\text{OH})_3$ because there is no obviously sharp structure at this position above the broad absorption envelope in the spectrum in [Figure 2d](#) from the $(\text{CH}_3\text{OH})_4\text{Na}^+$ mass channel. Of course, it is possible that ionization of a particular isomer of $\text{NaCl}(\text{CH}_3\text{OH})_4$ could generate $(\text{CH}_3\text{OH})_3\text{Na}^+$, but this isomer-selective ion fragmentation seems unlikely. This is confirmed by the PUCP data, which most closely match the $n = 3$ Poisson curve. The lowest-energy isomer of $\text{NaCl}(\text{CH}_3\text{OH})_3$ is expected to contain three equivalent IHBs, delivering two OH stretching bands because of the three-fold rotational symmetry in this structure. Guided by the DFT predictions, the band at 3278 cm^{-1} is assigned to the degenerate antisymmetric OH stretch. Other weaker absorption features are seen to the blue (and are also seen in the $(\text{CH}_3\text{OH})_2\text{Na}^+$ mass channel) at 3323 and 3349 cm^{-1} . These peaks are too weak to extract useful PUCP data, and therefore, we offer speculative assignments. Given the predicted splitting of 36 cm^{-1} , we assign the band at 3323 cm^{-1} to the symmetric OH stretch of

$\text{NaCl}(\text{CH}_3\text{OH})_3$, although once again this gives an experimental splitting (45 cm^{-1}) that is significantly larger than the DFT prediction. We have no specific assignment for the weak band at 3349 cm^{-1} (marked in Figure 2 with an asterisk) but speculate that it may arise from a higher-energy isomer of $\text{NaCl}(\text{CH}_3\text{OH})_3$ or possibly even from $\text{NaCl}(\text{CH}_3\text{OH})_4$.

There is a dramatic change in the IR spectra in going from detection of $(\text{CH}_3\text{OH})_3\text{Na}^+$ to $(\text{CH}_3\text{OH})_4\text{Na}^+$, as seen by comparing panels c and d in Figure 2. The spectrum in Figure 2d can only come from a complex with at least four methanol molecules and shows only very broad absorption features in the OH stretching region, extending from roughly 3100 through to 3400 cm^{-1} . A broad and largely structureless absorption in this region is also seen in the depletion spectrum recorded by detecting $(\text{CH}_3\text{OH})_5\text{Na}^+$ (not shown here). We attribute the broadening in the OH stretching region to the presence of overlapping bands from multiple isomers for $\text{NaCl}(\text{CH}_3\text{OH})_4$, as well as possible contributions from larger complexes owing to ion fragmentation. In support of this statement, the DFT calculations have found seven local minima within 3 kJ mol^{-1} of the global potential energy minimum of $\text{NaCl}(\text{CH}_3\text{OH})_4$, as illustrated in Figure 6. In Figure 2d, we show the predicted IR contributions from each of these isomers. No attempt has been made to employ a Boltzmann weighting to the relative contributions of the various isomers as this may not apply here, given that rapid cooling by the helium can trap molecules in metastable structures. However, the simulation does show that contributions from multiple isomers could span the observed absorption range and is therefore a plausible explanation for the spectral broadening.

4. Assignment of IR Spectra: CH Stretching. Clear bands are also seen from $\text{NaCl}(\text{CH}_3\text{OH})_n$ complexes in the CH stretching region. The CH stretching bands in Figure 2 are particularly strong for the spectra derived by detecting lighter $(\text{CH}_3\text{OH})_n\text{Na}^+$ ions, but there is also a recognizable trace of CH structure in the spectrum recorded at m/z 151 ($(\text{CH}_3\text{OH})_4\text{Na}^+$), which can only come from complexes with $n \geq 4$. The CH absorptions consist of three prominent bands at roughly 2830 , 2950 , and 2975 cm^{-1} , which are shifted a few cm^{-1} to the red of comparable bands in the isolated methanol molecule in liquid helium.¹⁹ By analogy with free methanol, these three bands can be assigned to the ν_3 , ν_9 , and ν_2 vibrations of the methanol units in $\text{NaCl}(\text{CH}_3\text{OH})_n$, respectively. The ν_3 mode is the symmetric CH stretch of the CH_3 group, while ν_9 and ν_2 are both antisymmetric CH stretches. These mode descriptions are approximate because multiple anharmonic couplings with overtone and combination states, such as $2\nu_{10}$ and $\nu_4 + \nu_{10}$, are well-known in this region.²¹ Indeed, a broad feature to the immediate red of the ν_9 band, which is most apparent in Figure 2b,c, probably reflects this additional vibrational complexity.

The fact that there is no significant change in the CH stretching structure in Figure 2 as the mass channel is changed suggests that the methyl group has no role in the binding of NaCl to methanol. This is entirely consistent with the theoretical predictions for the global minima, where binding of CH_3OH is dominated by IHBs and where there is no involvement of the methyl group. However, the DFT calculations do not do a particularly good job at predicting the positions of the CH stretching bands, in part because the scaling factor chosen is optimum for the OH stretching modes. Also, the intensities of the CH stretching bands in the experimental spectra relative to the OH stretches are

considerably higher than the DFT predictions, suggesting deficiencies in the particular DFT model employed here.

CONCLUSIONS

IR spectra have been recorded for $\text{NaCl}(\text{CH}_3\text{OH})_n$ complexes for the first time. Discrete vibrational bands are seen in the OH and CH stretching regions for $n = 1-3$. The positions of the OH stretching bands are consistent with formation of a dominant isomer in which the chloride ion undergoes an IHB to the OH group in each methanol molecule. This contrasts with $\text{Cl}^-(\text{CH}_3\text{OH})_n$ ions, where isomers with cooperatively enhanced IHBs have been seen for $n \geq 2$.²⁰ For $n \geq 4$, the discrete bands in the OH stretching region are replaced by broad absorption envelopes. This marked change in the spectra suggests that multiple isomers form for $n \geq 4$ in the liquid helium environment.

ASSOCIATED CONTENT

Supporting Information

The Supporting Information is available free of charge on the ACS Publications website at DOI: 10.1021/acs.jpca.6b06227.

Calculated vibrational frequencies and IR absorption line strengths and the IR spectrum recorded in the m/z 23 mass channel (PDF)

AUTHOR INFORMATION

Corresponding Authors

*E-mail: sfy1@le.ac.uk. Tel. +44 116 252 2138 (S.Y.).

*E-mail: andrew.ellis@le.ac.uk. Tel. +44 116 252 2138 (A.M.E.).

Notes

The authors declare no competing financial interest.

ACKNOWLEDGMENTS

The authors are grateful to the Leverhulme Trust (RPG-2012-740) and the UK Engineering and Physical Sciences Research Council (EP/L50502X/1) for grants in aid of this work. Support from the University of Nottingham for access to its High-Performance Computing facility and the Ministry of Higher Education and Scientific Research in Iraq for a Ph.D. studentship for A.M.S. are also gratefully acknowledged.

REFERENCES

- (1) Eisenberg, B. Ionic Interactions Are Everywhere. *Physiology* **2013**, *28*, 28–38.
- (2) Ault, B. S. Infrared spectra of argon matrix-isolated alkali halide salt/water complexes. *J. Am. Chem. Soc.* **1978**, *100*, 2426–2433.
- (3) Mizoguchi, A.; Ohshima, Y.; Endo, Y. Microscopic Hydration of the Sodium Chloride Ion Pair. *J. Am. Chem. Soc.* **2003**, *125*, 1716–1717.
- (4) Mizoguchi, A.; Ohshima, Y.; Endo, Y. The study for the incipient solvation process of NaCl in water: The observation of the $\text{NaCl}-(\text{H}_2\text{O})_n$ ($n = 1, 2, \text{ and } 3$) complexes using Fourier-transform microwave spectroscopy. *J. Chem. Phys.* **2011**, *135*, 064307.
- (5) Tandy, J.; Feng, C.; Boatwright, A.; Sarma, G.; Sadoon, A.; Shirley, A.; Das Neves Rodrigues, N.; Cunningham, E.; Yang, S.; Ellis, A. M. Infrared spectroscopy of salt-water complexes. *J. Chem. Phys.* **2016**, *144*, 121103.
- (6) Pinho, S. P.; Macedo, E. A. Solubility of NaCl, NaBr, and KCl in Water, Methanol, Ethanol, and their Mixed Solvents. *J. Chem. Eng. Data* **2005**, *50*, 29–32.
- (7) Li, M.; Constantinescu, D.; Wang, L.; Mohs, A.; Gmehling, J. Solubilities of NaCl, KCl, LiCl, and LiBr in Methanol, Ethanol,

Acetone, and Mixed Solvents and Correlation Using the LIQUAC Model. *Ind. Eng. Chem. Res.* **2010**, *49*, 4981–4988.

(8) Butler, J. A. V.; Thomson, D. W. The Behaviour of Electrolytes in Mixed Solvents. Part V. The Free Energy of Lithium Chloride in Water-Alcohol Mixtures and the Salting-Out of Alcohol. *Proc. R. Soc. London, Ser. A* **1933**, *141*, 86–94.

(9) Jungwirth, P. Hofmeister Series of Ions: A Simple Theory of a Not So Simple Reality. *J. Phys. Chem. Lett.* **2013**, *4*, 4258–4259.

(10) Bowron, D. T.; Finney, J. L. Anion Bridges Drive Salting Out of a Simple Amphiphile from Aqueous Solution. *Phys. Rev. Lett.* **2002**, *89*, 215508.

(11) Paschek, D.; Geiger, A.; Hervé, M. J.; Suter, D. Adding salt to an aqueous solution of *t*-butanol: Is hydrophobic association enhanced or reduced? *J. Chem. Phys.* **2006**, *124*, 154508.

(12) Shepperson, B.; Tandy, J.; Boatwright, A.; Feng, C.; Spence, D.; Shirley, A.; Yang, S.; Ellis, A. M. Electronic spectroscopy of toluene in helium nanodroplets: evidence for a long-lived excited state. *J. Phys. Chem. A* **2013**, *117*, 13591–13595.

(13) Lester, J. E.; Somorjai, G. A. Studies of the Evaporation Mechanism of Sodium Chloride Single Crystals Studies of the Evaporation Mechanism of Sodium Chloride Single Crystals. *J. Chem. Phys.* **1968**, *49*, 2940–2949.

(14) Shao, Y.; Gan, Z.; Epifanovsky, E.; Gilbert, A. T. B.; Wormit, M.; Kussmann, J.; Lange, A. W.; Behn, A.; Deng, J.; Feng, X.; et al. Advances in molecular quantum chemistry contained in the Q-Chem 4 program package. *Mol. Phys.* **2015**, *113*, 184–215.

(15) Zhao, Y.; Truhlar, D. G. The M06 suite of density functionals for main group thermochemistry, thermochemical kinetics, non-covalent interactions, excited states, and transition elements: two new functionals and systematic testing of four M06-class functionals and 12 other functionals. *Theor. Chem. Acc.* **2008**, *120*, 215–241.

(16) Scott, A. P.; Radom, L. Harmonic Vibrational Frequencies: An Evaluation of Hartree–Fock, Møller–Plesset, Quadratic Configuration Interaction, Density Functional Theory, and Semiempirical Scale Factors. *J. Phys. Chem.* **1996**, *100*, 16502–16513.

(17) Lin, C. Y.; Gilbert, A. T. B.; Gill, P. M. W. Calculating molecular vibrational spectra beyond the harmonic approximation. *Theor. Chem. Acc.* **2008**, *120*, 23–35.

(18) Raston, P. L.; Douberly, G. E.; Jäger, W. Single and double resonance spectroscopy of methanol embedded in superfluid helium nanodroplets. *J. Chem. Phys.* **2014**, *141*, 044301.

(19) Cabarcos, O. M.; Weinheimer, C. J.; Martínez, T. J.; Lisy, J. M. The solvation of chloride by methanol—surface versus interior cluster ion states. *J. Chem. Phys.* **1999**, *110*, 9516–9526.

(20) Beck, J. P.; Lisy, J. M. Cooperatively Enhanced Ionic Hydrogen Bonds in $\text{Cl}^-(\text{CH}_3\text{OH})_{1-3}\text{Ar}$ Clusters. *J. Phys. Chem. A* **2010**, *114*, 10011–10015.

(21) Gruenloh, C. J.; Florio, G. M.; Carney, J. R.; Hagemester, F. C.; Zwier, T. S. C-H Stretch Modes as a Probe of H-Bonding in Methanol-Containing Clusters. *J. Phys. Chem. A* **1999**, *103*, 496–502.